

Interference Alignment: Practical Challenges and Test-bed Implementation

†Nima Najari Moghadam, †Hamed Farhadi, †Per Zetterberg, *Majid Nasiri Khormuji, and †Mikael Skoglund

† ACCESS Linnaeus Center, KTH Royal Institute of Technology, Stockholm, Sweden

Emails: {nimanm, farhadih, perz, skoglund}@ee.kth.se,

*Huawei Technologies Sweden AB, Stockholm, Sweden, Email: majid.nk@huawei.com.

I. INTRODUCTION

Data traffic over wireless communication networks has experienced a tremendous growth in the last decade, and it is predicted to exponentially increase in the next decades [1]. Enabling future wireless networks to fulfill this expectation is a challenging task both due to the scarcity of radio resources (e.g. spectrum and energy), and also the inherent characteristics of the wireless transmission medium. Wireless transmission is in general subject to two phenomena: *fading* and *interference*. The former is a consequence of reflectors scattered in the environment surrounding a transmitter and a receiver such that the receiver observes a superposition of multiple copies of the transmitted signal. The superposition of the signals can be either constructive or destructive depending on the phase shift and attenuation of the received signals from different paths. The randomness of fading may degrade communication quality. Several effective techniques have been developed to overcome the adverse effects of random fading. For instance, multiple antennas transmission techniques are proposed to realize spatial diversity and to improve the performance of wireless systems in the presence of fading [2]. In addition, in multi-user networks because of the broadcast nature of wireless transmission medium, each user's communication is interfered by other users. Inter-user interference can severely degrade the communication quality and makes communication of different users interrelated; thus, finding the optimum interference management strategy becomes a challenging problem.

Conventional interference management strategies including time-division multiple access (TDMA) and frequency-division multiple-access (FDMA) avoid the inter-user interference by allocating orthogonal resources in time and frequency to different users, respectively. Interference is consequently avoided at the cost of low spectral efficiency. Thus, it was believed that the performance of wireless networks is limited by interference in general. However, the elegant *interference alignment* concept [3], [4] reveals that with proper transmission signalling design, different interference signals can in fact be aligned together, such that more radio resources can be assigned to the desired transmission. For instance, in the case of a multi-user interference network with more than two source–destination pairs, the interference signals at each destination can be aligned such that maximally half of the signal space can be left to its desired signal [4]. Therefore, each user may achieve half of the interference-free transmission rate no matter how many interferers exist [4]. Although interference alignment can achieve a larger data rate compared to orthogonal transmission strategies, several challenges should be addressed to enable the deployment of this technique in future wireless networks [1], [5]. For instance, to perform interference alignment, normally, global channel state information (CSI) is required to be perfectly known at all terminals. Clearly, acquiring such channel knowledge is a challenging problem in practice and proper channel training and channel state feedback techniques need to be deployed. In addition, since the channels are time-varying proper adaptive transmission is needed.

To investigate whether the outstanding performance of signal processing algorithms inspired by interference alignment can be preserved in real environment, practical verifications is needed. Wireless test-beds (e.g. the ones based on USRP or WARP) can be used as a platform for the experimental verification of the novel interference management algorithms.

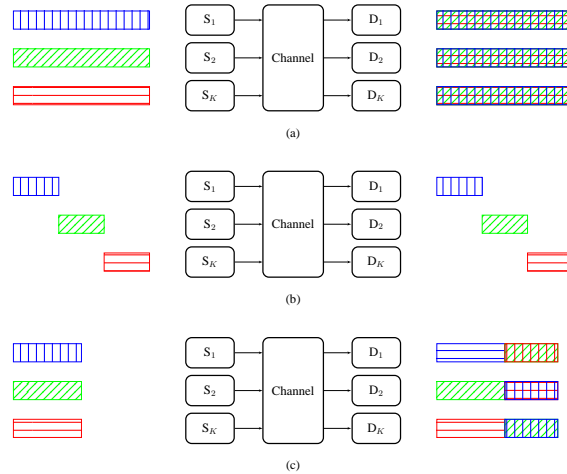


Fig. 1: Transmission schemes in three-user interference networks: (a) non-orthogonal transmission and decoding by treating interference as noise, (b) orthogonal transmission, and (c) interference alignment.

This chapter review recent advances in practical aspects of interference alignment. It also presents recent test-bed implementations of signal processing algorithms for the realization of interference alignment. In Section II we give a brief overview on the interference alignment concept. Section III presents the structure of a canonical transmitter and receiver to realize interference alignment, and discuss channel training and channel state feedback for these systems. A brief review on test-bed implementations of interference alignment solutions is presented in Section IV. Section V, introduces hardware and software setup of the test-bed used in this chapter for implementation of interference alignment. The test-bed implementation of iterative transceiver design and power control algorithm is presented in Section VI. We discuss the test-bed implementation of compressed feedback scheme for interference alignment scheme in Section VII. Finally, Section VIII concludes the chapter.

II. K -USER ($K > 2$) INTERFERENCE NETWORKS

Consider a K -user ($K > 2$) interference network. Several techniques have been devised for interference management in multi-user interference networks. Three major approaches to deal with interference are illustrated in Fig. 1. In Fig. 1 (a) all sources simultaneously transmit their signals in the same frequency band. Each source applies the conventional single-user coding technique. At each destination, the desired signal is superimposed by interference signals. The destination performs decoding by treating the interference signals as noise. This strategy is reasonable for cases that the receiver only knows the transmitted codebooks of the intended source. In the low signal-to-noise ratio (SNR) region, the level of interference can be controlled by proper power control techniques. However, in the high-SNR regime, inter-user interference is dominant. Therefore, the power control alone is not sufficient to manage the interference and this transmission strategy may not lead to a desirable performance.

The conventional approach to avoid interference at destinations is to orthogonalize the transmissions of different users. Each source–destination pair has access to only a portion of the available channel, as shown in Fig. 1 (b). Although signal reception at each destination does not directly suffer from inter-user interference, this scheme is not spectrally efficient due to the fact the resource; i.e. time or bandwidth, are divided among the source–destination pairs. From Fig. 1 (b), we see that the interference signals span a large dimension of the received signal space at each destination to ensure orthogonal reception. However, if at each destination the dimension of the subspace occupied by only the interference signals can be reduced, a larger interference-free subspace would be left for desired transmission. This can be realized using a new technique

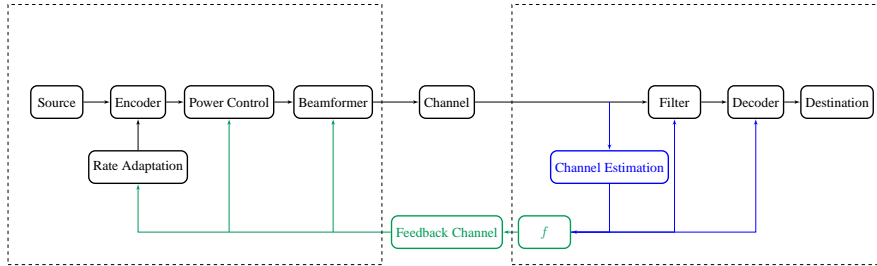


Fig. 2: Transmitter and Receiver Structure.

called *interference alignment* [3]. Specifically, interference alignment for interference networks refers to “a construction of signals in such a manner that they cast overlapping shadows at the receivers where they constitute interference while they remain distinguishable at the intended receivers where they are desired” [4]. In general, two conditions should be satisfied to perform interference alignment technique. First, interference signals should be aligned at the same subspace, termed *interference subspace*. Next, we need to check whether the subspace left for the desired signal, called *desired subspace*, is independent from the interference subspace. The conditions are essentially required for the realization of the interference alignment techniques. An illustrative representation of this concept is shown in Fig. 1 (c).

Interference alignment can be realized in different domains such as space (across multiple antennas [3], [4]), time (exploiting propagation delays [6], [7] or coding across time-varying channels [4], [8]), frequency (coding across different carriers in frequency-selective channels [9]), and code (aligning interference in signal levels [10]). Combinations of domains can also be used e.g. space and frequency, [11]. In the following, we briefly introduce *Degrees of Freedom (DoF)* which is a performance measure for wireless networks at high-SNR regime.

A. Degrees of Freedom Region

Consider the K -user interference network in Fig. 1. Source S_k ($k \in \{1, 2, \dots, K\}$) intends to send an independent message $w_k \in \mathcal{W}_k$ to its destination, where \mathcal{W}_k denotes the corresponding message set. The message w_k is encoded to a codeword of length n . Thus, the corresponding code rate is $R_k = \frac{\log |\mathcal{W}_k|}{n}$, where $|\mathcal{W}_k|$ denotes the cardinality of \mathcal{W}_k . The rate tuple (R_1, R_2, \dots, R_K) is said to be achievable if a sequence of codebooks exists, such that the probability that each destination decodes its message in error can be arbitrarily small, by choosing long enough codewords. The capacity region of the network is the closure of the set of all achievable rates. In Gaussian interference networks where the noise is additive white Gaussian, the capacity region depends on the transmission powers of sources, the noise powers and channel gains. Since the exact capacity region is difficult to find, as a starting point one can use the DoF region to characterize/approximate the capacity/achievable rate region in the high-SNR region (where interference is the dominant phenomenon that degrades system performance). The DoF region is defined as follows

$$\mathcal{D} = \left\{ (d_1, \dots, d_K) \in \mathbb{R}^+ \mid \exists (R_1, \dots, R_K) \in \mathcal{C}(P), d_k = \lim_{P \rightarrow \infty} \frac{R_k}{\log P}, 1 \leq k \leq K \right\}, \quad (1)$$

where $\mathcal{C}(P)$ denotes the capacity region, and P is the transmission power of each source. The DoF can be seen as the pre-log factor of the achievable rate and the DoF region describes how the capacity region expands as transmission power increases.

III. PRACTICAL CHALLENGES OF INTERFERENCE ALIGNMENT

The structure of a canonical transmitter and receiver for the implementation of interference alignment is shown in Fig. 2. At the transmitter side, there is an *encoder* which encodes the messages to the corresponding codewords suitable for

transmission over the channel. The transmission can be enhanced by the adaptation of the transmitted signal according to the received channel state information feedback. Specifically, in a class of communication systems that transmission powers are fixed and a maximum throughput is desired, the encoder may adapt transmission rate according to the estimate of the mutual information of the channel (computed by the *rate adaptation* module). On the other hand, in another class of systems which desire fixed-rate transmission, *power control* module should adjust transmitted power according to the channel state feedback to maintain mutual information of the channel larger than a certain level. Each transmitter has a *beamformer* which compute the proper signal for transmission over the channel according to the interference alignment concept.

At the receiver side, *channel estimation* module computes the estimation of incoming channel gains. These channel estimations can be used for recovering the transmitted message and computing the channel state information feedback signal. The *filter* module exploits estimated channel gains to recover the desired signal from interference signals according to the interference alignment concept. The *decoder* module decodes the message using an estimate of the incoming channel gain. The feedback encoder module denoted by ‘*f*’ in Fig. 2 computes the feedback signal according to the estimated channel gains. Also, there is a *synchronizer* module at the receiver to synchronize the receiver and the transmitter. In the following, we will explain these parts in more detail.

A. Channel Training for Interference Alignment

In practice, destinations can acquire CSI through a pilot-based channel training scheme. For example, consider block fading channel model in which channel gains are constant within one fading block and change to independent values in the subsequent blocks. The length of each block coincides with the coherence time of channel denoted as T .

Terminals first need to learn the channels within each fading block, and next use the estimated channels to perform their transmission. A pilot-assisted interference alignment scheme is proposed in [12] which perform these tasks. According to this scheme, transmission within each fading block is conducted in two phases: *pilot transmission phase* and *data transmission phase*. These two phases have the duration of $T_\tau = \alpha T$ and $T_d = (1 - \alpha)T$, respectively, where $\alpha \in [K/T, 1]$ called *channel sharing factor* is a design parameter. A larger α leads to more accurate channel estimation at the expense of less time left for data transmission. The transmission power of the pilot symbols in general can be different from that of the data symbols. Let P , P_d , and P_τ denote the average transmission power, the average power of data symbols, and the average power of pilot symbols, respectively. Source S_l ($l \in \{1, \dots, K\}$) sends T_τ known pilot symbols with power P_τ . Then, the destination D_k ($k \in \{1, \dots, K\}$) applies a minimum mean square error (MMSE) estimator to obtain an estimate of the channel gain. As shown in Fig. 2 this channel estimate is used at the receiver filter and the decoder to recover the desired message [13].

A more accurate estimation of the channel can be obtain by allocating more transmission power for training symbols which implies that a lower power is left for data transmission. The achievable rate region by taking into account this noisy CSI is computed in [12]. According to Proposition 2 in [12], the optimum power allocation which maximizes the achievable rate region is

$$\begin{aligned} P_{d,\text{opt}} &= \beta_{\text{opt}} P, \\ P_{\tau,\text{opt}} &= K ((1 - (1 - \alpha) \beta_{\text{opt}}) / \alpha) P, \end{aligned} \quad (2)$$

where

$$\beta_{\text{opt}} = \frac{1}{1 - \alpha} \left(1 + \sqrt{\frac{1 + KP/(1 - \alpha)}{1 + PT/N_0}} \right)^{-1}. \quad (3)$$

If $P \gg 1$, then the optimum power allocation factor is approximately

$$\beta_{\text{opt}} \approx \frac{1/(1 - \alpha)}{1 + \sqrt{KN_0/T(1 - \alpha)}}. \quad (4)$$

This result recommends that in large networks more power should be allocated to the channel training instead of the data transmission. The intuition behind this result is that in large networks the performance loss due to imperfect interference alignment as a consequence of imperfect CSI becomes more important. Thus, it is recommended to allocate more power to pilot symbols instead of data symbols to acquire CSI more accurately.

B. Channel State Information Feedback

As we have discussed in the previous section, destinations can acquire CSI through a pilot-based channel training scheme. The destinations then can send the estimated CSI to the sources via channel state feedbacks. They can transmit either unquantized CSI (analog feedback) or quantized CSI (digital feedback) via feedback channels. In the following, we briefly review some key results for different type of feedback schemes.

1) *Analog Feedback*: The destinations can obtain an estimate of the incoming channels according to the scheme mentioned in Section III-A. Then, they may transmit the analog value of the estimated channels over the feedback channel. Let the function f in Fig. 2 to be defined as $f(x) = x$, and assume error-free feedback channels. According to Theorem 3 in [12], in a single-input single-output (SISO) time-varying K -user network with coherence time T , the achievable sum DoF is

$$d_{\Sigma} = \min\{K(1 - K/T)/2, T/8\}. \quad (5)$$

This result is achieved when the number of the users selected to be active is

$$K_{opt} = \min\{K, T/2\}. \quad (6)$$

This recommends that, in large networks ($K > T/2$) when no CSI is a priori available at terminals, first select a subset of the users and next perform channel training and interference alignment within the set of active users.

2) *Digital Feedback*: Digital channel state feedback strategies in which each destination quantize the incoming channels and sends the index of the quantized channel over feedback channels has been studied in several works (e.g. [14]–[16]). It is shown that the same DoF as when perfect CSI is available can be obtained, provided that the destinations a priori know channels and the feedback signals' rate is proportional to $\log P$, where P is the transmission power of each source. That is,

$$N_f \sim \log P, \quad (7)$$

where N_f is the number of feedback bits. It should be noticed that in practice where destinations do not know incoming channels a priori, part of the radio resources need to be allocated for channel training and a smaller DoF will be achievable (cf. [12]). This part is discussed in more detail in section VII-A.

C. Iterative Interference Alignment

In this part we present an iterative algorithm referred to as *leakage minimization algorithm* and an extension for it called *Max-SINR* which both are proposed in [17]. Consider a three-user multiple-input multiple-output (MIMO) interference network where each terminal is equipped with M antennas. For presentation simplicity here we assume M to be even. The result when M is odd is provided in [4]. It has been shown in [4] that the achievable DoF of each source–destination pair is $\frac{M}{2}$. To achieve this DoF, the transmitter-side beamformers and the receiver-side filters should be designed. In the following, we will briefly present the algorithm proposed in [17] to compute the beamformers and filters. We assume each terminal can acquire only local channel side information, i.e. knowledge about the channels which are directly connected to it through out training of the channel. Destination D_k can obtain \mathbf{H}_{kl} and source S_k can obtain \mathbf{H}_{lk} , $l \in \{1, 2, 3\}$, where \mathbf{H}_{lk} is the forward channel from S_k to D_l and \mathbf{H}_{kl}^T is the reverse channel from D_l to S_k . The iterative computation of the beamformers and the filters occur in the training phase. After the convergence of the computed filters and beamformers to

the interference alignment solutions, the data transmission starts. Let \mathbf{V}_k denote an $M \times \frac{M}{2}$ transmitter-side beamforming matrix where its columns are the orthogonal basis of the transmitted signal space of S_k . The transmitted signal of S_k is

$$\mathbf{x}_k = \mathbf{V}_k \bar{\mathbf{x}}_k, \quad (8)$$

where each element of the $\frac{M}{2} \times 1$ vector $\bar{\mathbf{x}}_k$ represents an independently encoded Gaussian codeword with power $\frac{2P_k}{M}$. Each codeword is beamformed with the corresponding column of \mathbf{V}_k .

Let \mathbf{U}_k be an $M \times \frac{M}{2}$ receiver-side filtering matrix whose columns are the orthogonal basis of the desired signal subspace at D_k . The filter output of D_k is

$$\bar{\mathbf{y}}_k = \mathbf{U}_k^* \mathbf{y}_k, \quad (9)$$

where \mathbf{y}_k is the received vector. The transmitter-side beamforming matrices and the receiver-side filtering matrices should satisfy the following interference alignment conditions:

$$\begin{aligned} \mathbf{U}_k^* \mathbf{H}_{kj} \mathbf{V}_j &= 0, \quad \forall j \neq k : j, k \in \{1, 2, 3\}, \\ \text{rank}(\mathbf{U}_k^* \mathbf{H}_{kk} \mathbf{V}_k) &= \frac{M}{2}, \quad \forall k : k \in \{1, 2, 3\}. \end{aligned} \quad (10)$$

If global CSI is available, the beamforming and filtering matrices can be designed such that these conditions are satisfied. However, with the lack of global CSI if we choose the beamformers and the filters randomly, with high probability only the second condition in (10) will be satisfied. Consequently, some interference remains at the destinations. The total power of interference at D_k is

$$IF_k = \text{Tr}[\mathbf{U}_k^* \mathbf{Q}_k \mathbf{U}_k], \quad (11)$$

where

$$\mathbf{Q}_k = \sum_{j=1, j \neq k}^3 \frac{2P_j}{M} \mathbf{H}_{kj} \mathbf{V}_j \mathbf{V}_j^* \mathbf{H}_{kj}^* \quad (12)$$

is the covariance matrix of interference at D_k . Clearly, $IF_k = 0$ only if the beamformers and the filters satisfy conditions in (10). However, D_k can utilize the local channel side information to minimize this received interference power by optimizing its receiver-side filter. Therefore, assuming that the beamformers are fixed, the receiver-side filter \mathbf{U}_k is the solution of the following problem:

$$\min_{\mathbf{U}_k, \mathbf{U}_k \mathbf{U}_k^* = \mathbf{I}_{\frac{M}{2}}} IF_k. \quad (13)$$

The solution is given in [17]:

$$\mathbf{U}_k^d = \nu^d[\mathbf{Q}_k], \quad d = 1, \dots, \frac{M}{2}, \quad (14)$$

where \mathbf{U}_k^d denotes the d th column of \mathbf{U}_k and $\nu^d[\mathbf{A}]$ is the eigenvector corresponding to the d th lowest eigenvalue of \mathbf{A} .

To optimize the transmitter-side beamformers the reciprocity of the channels can be exploited to obtain CSI at sources. For instance, destinations can transmit training sequences over the *reverse channels* (channels from destinations to sources) which are separated from the *forward channels* (channels from sources to destinations) in time via time-division duplex (TDD). The *reciprocity* of the forward and reverse channels is assumed, i.e. $\mathbf{H}_{kl}^r = \mathbf{H}_{lk}^* (\forall l, k \in \{1, 2, \dots, K\})$. For this purpose, the destination D_k performs beamforming and S_k perform filtering in the reverse direction with matrices \mathbf{V}_k^r and \mathbf{U}_k^r , respectively. These matrices can be selected to perform interference alignment in the reverse direction. Since, the reciprocity holds, if we choose $\mathbf{U}_k^r = \mathbf{V}_k$ and $\mathbf{V}_k^r = \mathbf{U}_k$, the solutions of the interference alignment problem in the reverse direction are equivalent to those in the forward direction. In a similar way as in the forward direction, the reverse direction

filters are computed as,

$$(\mathbf{U}_k^r)^d = \nu^d [\mathbf{Q}_k^r], \quad d = 1, \dots, \frac{M}{2}, \quad (15)$$

where \mathbf{Q}_k^r is the covariance matrix of interference at S_k and is computed in a similar way as in (12) with the reverse direction channels and beamformers. We can set the beamforming matrices in the forward direction as $\mathbf{V}_k = \mathbf{U}_k^r$ and repeat this optimization procedure until the beamforming matrices and the receiving filters converge. The convergence of this algorithm is shown in [17]. Next, the sources beamform their data using the computed beamforming matrices and the destinations decode their desired signals by applying associated filters.

An extension of this iterative algorithm is proposed in [17] which instead of minimizing leakage at each destination tries to maximize signal-to-noise-plus-interference ratio (SINR) corresponding to each stream. This algorithm is referred to as *Max-SINR algorithm* in the literature. According to *Max-SINR algorithm*, the receiver filtering vector \mathbf{U}_k^d instead of the one in (14) is selected to be a MMSE filter as follows

$$\mathbf{U}_k^d = \frac{(\mathbf{Q}_k^d)^{-1} \mathbf{H}_{kk} \mathbf{V}_k^d}{\|(\mathbf{Q}_k^d)^{-1} \mathbf{H}_{kk} \mathbf{V}_k^d\|_2}, \quad (16)$$

where

$$\mathbf{Q}_k^d = \sum_{j=1}^K \sum_{l=1}^{M/2} \frac{2P_j}{M} \mathbf{H}_{kj} \mathbf{V}_j^l (\mathbf{V}_j^l)^* \mathbf{H}_{kj}^* - \frac{2P_j}{M} \mathbf{H}_{kk} \mathbf{V}_k^d (\mathbf{V}_k^d)^* \mathbf{H}_{kk}^* + N_0 \mathbf{I}_{M/2}. \quad (17)$$

where $\mathbf{I}_{M/2}$ is $\frac{M}{2} \times \frac{M}{2}$ identity matrix and N_0 is the noise power. Similarly, the transmitter beamforming vectors are updated in the reverse transmissions. In the following sections, we will present test-bed implementation of algorithms which use Max-SINR algorithm for computing the transmitter and receiver filters.

IV. REVIEW ON TEST-BED IMPLEMENTATION OF INTERFERENCE ALIGNMENT

The idea of squeezing aligned interference signals into half of the signal space and accessing the other half of the signal space for desired transmission in an interference network is so tempting that a large body of works has been done since the introduction of interference alignment to implement this elegant approach, for instance look at [9], [18]–[26].

The first implementation of interference alignment is reported in [18]. A hybrid version of interference alignment combined with the successive interference cancellation (IAC) in a single carrier narrow-band MIMO wireless local area network (WLAN) is tested in this paper. Several interference alignment and interference alignment-like approaches are tested in MIMO-OFDM interference channels in [19]. This paper specifically studies the effects of poor channel conditions on the performance of interference alignment. Real-time implementation of different interference alignment scenarios are performed on different test-beds like the ones in [21]–[23]. [21] identifies practical issues that degrades the interference alignment performance such as channel estimation errors or collinearity between the desired signal and interference subspaces while in [23], in Vienna MIMO test-bed (VMTB), the typical delay is measured.

Implementation of interference alignment in frequency domain over measured channels is considered in [9] where the different variants of interference alignment are compared with frequency planning scenarios. The significant superiority of interference alignment performance in terms of average sum rate is reported at high SNRs in this paper.

In all previously mentioned papers, the effects of hardware impairments are ignored. In [20], the effects of such impairments on the performance of interference alignment and coordinated multi-point¹ (CoMP) is investigated on *KTH four-multi* test-bed and a measurement based model for signal-to-interference-noise-and-distortion ratio (SINDR) is suggested. Implementation of interference alignment with power control and interference alignment with compressed feedback are also

¹CoMP is an approach similar to interference alignment with this main difference that in CoMP all the sources know the information to be transmitted to all destinations.

studied on the same test-bed in [24] and [25], respectively. These two approaches are further explained in the rest of this chapter. Table below summarizes some of the works that have been done in the test-bed implementation of interference alignment.

Reference	alignment dimension	implemented algorithms	number of user pairs	channels	DL/UL	antennas per node	hardware	f_c (GHz)	synchronization	Measurement environment
[18]	Space	IA in DL IAC in UL	2 and 3	flat-fading MIMO	DL and UL	2	USRP (one per node)	–	–	indoor office
[19]	Space	variants of IA	3	MIMO-OFDM	DL	2	NI PXI-1045	2.4	high precision OCXO software correction trigger signal	indoor and outdoor
[20]	Space	MAX-SINR	3	MIMO-OFDM	DL	2	USRP	2.49	10 MHz CLK NMEA PPS	indoor office
[9]	Frequency	variants of IA	3	measured SISO-OFDM	DL	1	LTE BS	2.7	N/A	urban macrocell
[21]	Space	IA	3	MIMO-OFDM	DL	2	Lyrtech	5	40 MHz OSC hardware trigger	indoor office
[22]	Space	IA	3	MIMO-OFDM	DL	2	USRP	2.4	10 MHz CLK PPS	indoor office
[23]	Space	IA	3 (1 physical and 2 virtual Rx)	MIMO-OFDM	DL	4	VMTB	2.503	rubidium CLK GPS	outdoor to indoor indoor to outdoor
[24]	Space	IA with PC	3	MIMO-OFDM	DL	2	USRP	2.4	10 MHz CLK NMEA PPS	indoor office
[22]	Space	IA with compressed feedback	3	MIMO-OFDM	DL	2	USRP	2.4	10 MHz CLK NMEA PPS	indoor office

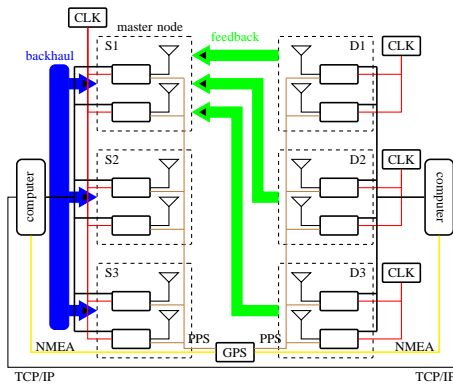


Fig. 3: Network structure of KTH four-multi test-bed.

V. KTH FOUR-MULTI TEST-BED SETUP

KTH four-multi is a USRP-based wireless communication test-bed consisting of several stationary and movable multi-antenna nodes. A software framework accompanies the hardware setup of the test-bed which facilitates the rapid testing of multi-antenna schemes (see <http://fourmulti.sourceforge.net/>). In the following, the hardware and software structure of the test-bed is described.

A. Hardware Setup

The current version of the test-bed consists of six nodes where three of them are fixed and take the role of transmitting sources while the other three are movable receiving destinations. All the nodes are equipped with two vertically polarized dipole antennas spaced 20 cm apart which is 1.6 times of the carrier's wavelength. Twelve Ettus Research USRP N210 (see www.ettus.com) are used to govern the twelve antennas in the network. The source USRPs are equipped with the standard Ettus XCVR2450 RF daughterboards while the destination USRPs use custom boards to achieve sufficient noise figure and dynamic range. The output signal of each source USRP is amplified by a ZRL-2400LN power amplifier. Two Linux computers control all the USRPs in the network. The network structure of four-multi test-bed is illustrated in Fig. 3.

The network is designed to work at 2.49 GHz center frequency with 12 MHz bandwidth. Synchronization of the network is performed in three levels, namely time, frequency and transmit-receive synchronizations. The time and transmit-receive synchronizations are done by means of a pulse-per-second (PPS) signal (0-5 V, 1 Hz square wave) and a national marine electronics association (NMEA) signal (an ASCII protocol that provides hour-minute-second time), respectively. Both signals are generated by an EM406A GPS module and distributed through the network. The frequency synchronization is also performed by helps of 10 MHz reference clocks (CLK). All the source's local oscillators are locked to the same clock while a separate clock is provided for each of the destinations. In a real implementation the same synchronization would be achieved using common control and synchronization channels (cellular systems) or from the burst preambles (wireless local area networks). In a system with interference alignment, transmitter will in any case need some kind of back-haul to provide a common time reference and disperse scheduling decisions.

B. Software Setup

The four-multi software framework has been developed in C++ (see <http://fourmulti.sourceforge.net/>). It run on two Linux computers separately. One of the computers controls the three source nodes while the other one controls the three

TABLE I: KTH four-multi modulation and coding toolbox specifications.

OFDM1		AMC	
FFT length	80	Coding rates	$\frac{1}{2}, \frac{5}{8}, \frac{3}{4}$
Cyclic prefix length	12	Codeword length	1520
Number of null subcarriers	42	QAM modulation orders	4, 16, 64, 256
Subcarrier spacing (KHz)	312.5		

destination nodes connected to them via Ethernet connections. The sources' computer generates the transmitted frames and feeds them to the source nodes while the destinations' computer process the received frames at the destination nodes. A TCP/IP connection between the source and the destination computers provides the feedback links. Backhaul communication among the source nodes is also implemented by the help of TCP/IP connections between the source computer and the source nodes.

The framework contains a toolbox for coding and modulation (AMC and OFDM1) which was used in the implementations of the next two sections. The modulation and coding toolbox includes an LDPC channel encoder/decoder, a QAM modulator/demodulator and an OFDM modulator/demodulator. The specifications of these built-in functions is summarized in Table I.

VI. TEST-BED IMPLEMENTATION OF THE ITERATIVE TRANSCIEVER FILTER DESIGN AND POWER CONTROL

We, in this section, first present an iterative algorithm for joint transceiver filter design and power control proposed in [27] and then explain how this algorithm is implemented on KTH four-multi test-bed and finally present measurement results.

A. Iterative Transceiver Filter Design and Power Control Algorithm

In an interference network, each user can affect the received SINR at its corresponding destination through the choice of beamforming and receiving filters as well as the transmitting power. Considering single stream transmissions, the received SINR at the k th destination is computed as

$$\text{SINR}_k(\mathbf{u}_k, \mathbf{v}_k, P_k) = \frac{P_k \mathbf{u}_k^* \mathbf{H}_{kk} \mathbf{v}_k \mathbf{v}_k^* \mathbf{H}_{kk}^* \mathbf{u}_k}{IF_k + N_0} \quad (18)$$

where IF_k is given by (11). Given the beamforming and receiving filters, from Equation (18) the minimum transmitting power required to maintain a fixed rate $R_{tar,k}$ (assuming that the interference can be regarded as Gaussian noise) at k th destination can be found as

$$P_k = \beta_k(\mathbf{u}_k, \mathbf{v}_k, \gamma_k) := \frac{\gamma_k (IF_k + N_0)}{\mathbf{u}_k^* \mathbf{H}_{kk} \mathbf{v}_k \mathbf{v}_k^* \mathbf{H}_{kk}^* \mathbf{u}_k}, \quad (19)$$

where $\gamma_k = 2^{R_{tar,k}} - 1$ is the minimum required SNR in an AWGN channel. The total power of the interference, IF_k which appears in the nominator is a function of transmitting powers at all the interfering transmitters. It means that increasing the power of one source causes higher level of interference at non-corresponding destinations and therefore the other sources need to transmit with higher power as well. In [28], it is shown that if the relation between the powers P_k , $k = 1, \dots, K$ satisfies a set of conditions then either there is a unique solution for the powers that can be found iteratively starting from any initial value or no solution exists. It is easy to prove that Equation (19) meets the conditions in [28] and therefore an optimal transmitting powers can be found distributively after a sufficient number of iterations.

Inspired by Max-SINR algorithm and the aforementioned power control algorithm, an iterative transceiver design and power control algorithm was proposed in [27]. A brief version of the algorithm is presented on the next page for the sake of completeness. The algorithm is composed of three update phases in each iteration such that the receiving filters,

Algorithm 1 Transceiver Filter Design and Power Control [27]

Initialize: $\mathbf{v}_k(0), P_k(0), k \in \{1, \dots, K\}, n = 1.$

repeat

Update receiver filtering vector:

$$\mathbf{u}_k(n) = \arg \max_{\mathbf{u}_k} \{\text{SINR}_k(\mathbf{u}_k, \mathbf{v}_k(n-1), P_k(n-1))\} \quad (20)$$

Update transmission power:

$$P_k(n) = \min \{\beta_k(\mathbf{u}_k(n), \mathbf{v}_k(n-1), \gamma_k), P_{\max}\} \quad (21)$$

Reverse the communication direction:

$$\begin{cases} \mathbf{u}_k^r(n-1) = \mathbf{v}_k(n) \\ \mathbf{H}_{ij}^r = \mathbf{H}_{ji}^* & i, j \in \{1, \dots, K\} \\ P_k^r(n-1) = P_F \end{cases}$$

Update transmitter beamforming vector:

$$\mathbf{u}_k^r(n) = \arg \max_{\mathbf{u}_k^r} \{\text{SINR}_k^r(\mathbf{u}_k^r, \mathbf{v}_k^r(n-1), P_k^r(n-1))\} \quad (22)$$

Set beamforming vector $\mathbf{v}_k(n) = \mathbf{u}_k^r(n)$, and $n = n + 1.$

until $n = N$

transmission powers and beamforming filters are sequentially updated. The receiving and beamforming filters are optimized to deliver the maximum SINR at the destinations in the forward communication direction and at the sources in the reverse direction, respectively according to the concept of Max-SINR algorithm. On the other hand, in the power update phase, the powers are set to the minimum values needed for maintaining a fixed rate communication. The transmission power is upper bounded by P_{\max} . This algorithm assumes that accurate CSI is obtained at terminals. An extensions of the algorithm when terminals have access to only noisy CSI is proposed in [29].

B. Transmitted Frame Structure

The air interface of the network is designed based on OFDM modulation using Four-multi's modulation and coding toolbox. Coding rate of 1/2 and 16QAM modulation was chosen for transmitting fixed-rate data streams through the air interface. The transmitted frame structure is depicted in Fig. 4. In our experiment, each frame consists of 20 payload symbols and either two or three reference signals (RS) (i.e. pilot symbols). The payload symbols are *concurrently* transmitted from all the sources while each stream is beamformed with its corresponding beamforming filter instructed by Algorithm 1. Although the overhead of pilot symbols is significant in this case, we note that the number of payload symbols could be larger depending on the coherence time of the indoor channel. In the implementation in Section VII there are in fact thousands of payload symbols with no additional pilots. Thus the overhead could be reduced to one percent for the environment in Fig. 5.

Three types of RS are employed in the network, which are referred to as *channel state information RS (CSI-RS)*, *demodulation RS (DM-RS)* and *power RS (P-RS)*. During the pilot transmission all the sub-carriers of the OFDM symbol is filled with known QAM symbols. We next explain each type of these reference signals:

- CSI-RS: The received noisy CSI-RS at the destinations are exploited to estimate the corresponding channel matrices to enable execution of Algorithm 1. The CSI-RS are transmitted *orthogonally*; i.e., one CSI-RS is transmitted from each

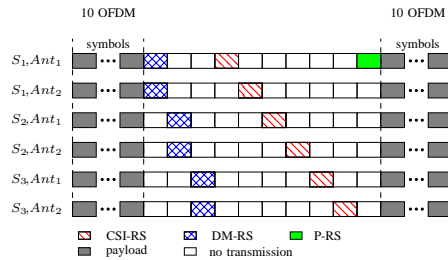


Fig. 4: Transmitted frame structure in IA-PC scheme.

transmit antenna in the network while the other antennas are silent. To enhance the quality of the channel estimations the CSI-RS are scaled such that the associated QAM symbol has the maximum transmit power P_{\max} .

- DM-RS: The DM-RS are used to compute the effective channel by taking into account the transmit and receive filters. Therefore they need to be stream-dedicated and be processed by the same pre-coder as the payload symbols of the corresponding stream. In this way, their power is not fixed and is set by the power control algorithm.
- P-RS: Algorithm 1 is constructed to select the minimum possible transmission power to minimize the interference at the destinations. This hence reduces the power of DM-RS and may lead to a poor estimation of cross-channels, which is not favorable. To tackle this problem, P-RS is introduced where the amplitudes of the DM-RS are scaled after the pre-coder by a scaling factor α . In each frame, the scaling factor is computed as

$$\alpha = \sqrt{\frac{P_{\max}}{\max_{k,j} P_{k,j}}}, \quad (23)$$

where $P_{k,j}$ is the transmit power of the j th sub-carrier of k th source. The destinations therefore need to get informed about the scaling factor. This is achieved by having node 1 (the master node) repeat its first CSI-RS but now scaled with α . This enables all destinations to make robust estimate of α (it is assumed that all destinations can hear node 1). The factor α is also quantized into a discrete set of values to avoid that α introduces estimation errors.

C. Measurement results

The test-bed measurement was performed in KTH signal processing department which floor map is illustrated in Fig. 5. The measurement environment is categorized as an indoor office. In this experiment only non-line-of-sight (non-LOS) scenarios were investigated by placing source and destination nodes in the corridor and inside the nearby offices, respectively. The receive antenna gains also decreased by connecting 10 dB attenuators to them in order to avoid saturation of receive power amplifiers.

The measurement was done in 100 batches. In each batch a random placement of the destination nodes in the area marked by colored circles in the figure were measured. The signals transmitted according to two different schemes were measured sequentially in each batch. In the first scheme, referred to as *noPC*, the iterative interference alignment was implemented according to [17] for benchmarking. In the second scheme, referred to as *PC*, transmission powers and beamforming filters were computed according to Algorithm 1 and MMSE receiving filters were applied at the destinations. Each scheme was run with 28 frames inter-spaced 0.15 seconds. The statistics of the first frames of both schemes were not taken into account since there is no feedback information at these frames.

High power may push the terminals' power amplifier to work in their non-linear region. Non-linearities in the transmit-receive chain degrades the performance of the system by introducing *distortion noise* into the system. Distortion noise is usually modeled as a Gaussian noise whose power increases by increasing the transmission power of the source nodes [30].

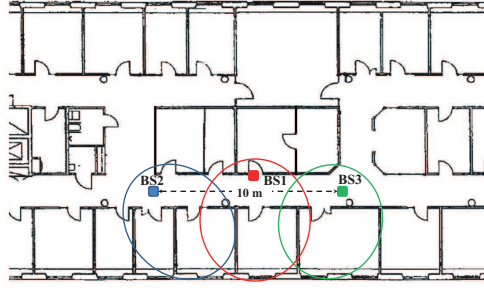


Fig. 5: Measurement environment map.

TABLE II: Measurement results.

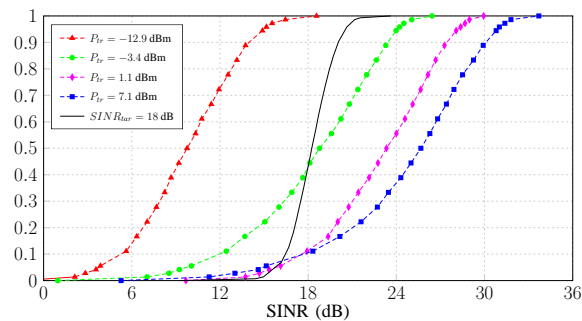
scheme	noPC				PC
Average power (dBm)	-12.9	-3.4	1.1	7.1	-1
FER	0.6856	0.1700	0.0528	0.0561	0.0071
BER	0.0815	0.0124	0.0020	0.0030	2.2×10^{-4}
Average SINR (dB)	10.9	20	24.3	26.7	18.5

In order to make sure that the reduction of transmit power is not the only cause for the performance improvement, four different levels of transmission power were tested in noPC scheme that is each 7 frames were transmitted with a different power.

Table II shows the average performance of the two schemes for the 100 measurement batches. In this measurement the PC scheme's target SINR γ_k was set to 18 dB for all the users. The performances were compared in the sense of bit-error rate (BER) and transmitted power. The table shows that the PC scheme has the lowest BER, although its average transmit power is much lower than the noPC scheme with the best BER performance.

Empirical cumulative distribution function (CDF) of the received SINR for two schemes is plotted in Fig 6. This plot reveals the reason for the low BER of PC scheme despite its low transmit power. The received SINRs in this scheme are concentrated around the target value while in the noPC scheme they are distributed over a wider range. Having SINR higher than the target value while the transmit rate is fixed leads to the waste of energy and on the other hand SINRs lower than the target increase the probability of error and therefore the BER.

Power saving gain at each frame is computed as the ratio of the transmit power in noPC scheme with 7.1 dBm average

Fig. 6: Empirical CDF of SINR. The solid line represents the PC scheme and the dashed lines denote the noPC scheme with different transmit powers (P_{tr}).

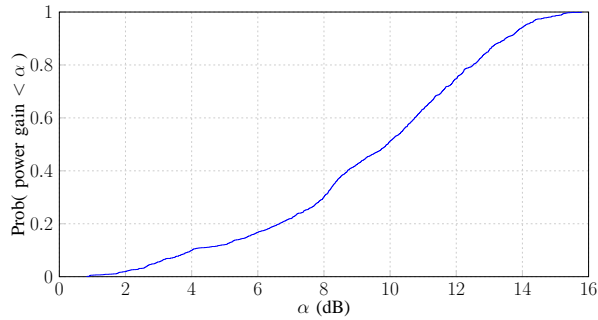


Fig. 7: Empirical CDF of transmit power saving gain.

power and the total power transmitted in the PC scheme with 18 dB target SINR. Fig. 7 shows the empirical CDF of the power saving gain. As the empirical CDF implies, implementation of Algorithm 1 in PC scheme leads to at least 4 dB gain in 90% of the measurements. Fig. 7 also shows that in 10% of the measurements gains higher than 13 dB was observed.

The benefit of power control in the PC scheme is in fact two-fold. By decreasing the transmit power, while retaining the target SINR, not only less interference is received at the destinations but also the distortion noise due to transceiver impairments decreases.

VII. TEST-BED IMPLEMENTATION OF THE INTERFERENCE ALIGNMENT WITH COMPRESSED FEEDBACK

In this section we describe the implementation of interference using limited digital feedback (see Section III-B2). Rather than using a uniform quantizer, we use a modified form of the MIMO matrix compression of the IEEE802.11ac standard. The propagation scenario and testbed is the same as the one used in Section VI i.e. a system with three ($K = 3$), 2×2 MIMO links. However, the transmission power is higher than in previous sections and the system is therefore limited by interference and hardware impairments rather than thermal noise [25], [26]. A second difference from the previously presented results in Section VI, is the performance criterion. Rather than using BER we here use transmission rate as the criterion. The transmission rate is obtained by probing each link with ten different coding and modulation schemes (MCS). The rate is determined by finding the MCS with the highest rate which does not incur any frame errors.

The section is organised as follows. Section VII-A describes the feedback compression of the CSI assuming a system with K links and M antennas in each source and destination node, while the measurement results are presented in Section VII-B.

A. Compression of IEEE802.11ac and adaptation to interference alignment

The feedback scheme described in the standard IEEE802.11ac resembles the feedback method for slowly time-varying single-user MIMO channels presented in [31]. In this scheme a singular value decomposition (SVD) of the MIMO channel \mathbf{H} (for a certain sub-carrier) is first performed as

$$\mathbf{H} = \mathbf{W}\mathbf{\Lambda}\mathbf{F}^*. \quad (24)$$

The destination then feeds back, in compressed form, the complex unitary matrix \mathbf{F} and the real diagonal matrix $\mathbf{\Lambda}$, while the complex unitary matrix \mathbf{W} does not need to be fed back. To realize this we may imagine that each destination pre-multiplies its received signal with \mathbf{W}^* . The effective channel then becomes $\check{\mathbf{H}} = \mathbf{\Lambda}\mathbf{F}^*$ which is a channel which can be reconstructed by the sources. In practice, the destination will not pre-multiply its received signal with \mathbf{W}^* , since almost every receive technique is invariant to such a linear unitary transform.

In the case of centralised interference alignment, knowledge of the channels between all sources and destinations is required to obtain all the beamformers \mathbf{V}_k . We assume here that sources are connected to a common back-bone for exchange of CSI and synchronization. If we directly apply the compression scheme presented above for the single-user case so that each destination D_k , compresses the matrices $\mathbf{H}_{k,l}$ for $l \in \{1, \dots, K\}$ it is clear that there is no single unitary matrix to be applied at the destination to transform all involved K channels into $\check{\mathbf{H}}_{k,l} = \mathbf{\Lambda}_{k,l} \mathbf{F}_{k,l}^*$ such that all channels can be obtained from the compressed feedback from user k .

To overcome this problem, in the system implementation we have based the feedback from destination k on the big matrix, $\mathbf{H}^{[k]}$ obtained by concatenating the channel matrices $\mathbf{H}_{k,l}$ for $l = 1, \dots, K$ column-wise. Thus in this case $\mathbf{H}^{[k]}$, is computed as,

$$\mathbf{H}^{[k]} = [\mathbf{H}_{k,1}, \dots, \mathbf{H}_{k,K}]. \quad (25)$$

Thus D_k now feeds back a compressed version of the right-hand side eigenvectors of $\mathbf{H}^{[k]}$ i.e. the real diagonal matrix $\mathbf{\Lambda}^{[k]}$ and the complex unitary matrix $\mathbf{F}^{[k]}$ of the SVD

$$\mathbf{H}^{[k]} = \mathbf{W}^{[k]} \mathbf{\Lambda}^{[k]} (\mathbf{F}^{[k]})^*. \quad (26)$$

The size of matrix $\mathbf{\Lambda}^{[k]}$ is $M \times M$ while $\mathbf{F}^{[k]}$ is $KM \times M$. Just as in the single-link case we can now imagine that the destination pre-multiplies its received signal with $(\mathbf{W}^{[k]})^*$. The transmitter side is then able to obtain knowledge of the effective channel $\check{\mathbf{H}}^{[k]} = \mathbf{\Lambda}^{[k]} (\mathbf{F}^{[k]})^*$. From this combined channel the constituent sub-channels can be pulled out from the corresponding columns e.g. the second channel $\check{\mathbf{H}}_{k,2}$ corresponds to columns $M+1, \dots, 2M$ of $\check{\mathbf{H}}^{[k]}$. The reconstructed channels can then be used in place of the actual channels in any transmit beamformer and receive filter algorithm.

The IEEE 802.11ac feedback compression scheme starts by rotating the phase of the columns of $\mathbf{F}^{[k]}$ in order the last row of this matrix to have real and positive elements. These phase rotations do not need to be sent to the sources, since these rotations only amount to a phase rotation of the signals which can be undone at the destination. In the next step, $\mathbf{F}^{[k]}$, is multiplied by a diagonal matrix to have the first column become real and positive as

$$\mathbf{F}^{[k]} \leftarrow \mathbf{F}^{[k]} \mathbf{diag}(\exp(j\phi_{1,1}), \dots, \exp(j\phi_{KM-1,1}), 1). \quad (27)$$

These angles $\phi_{1,1}, \dots, \phi_{KM-1,1}$ are then quantised uniformly, each with b_ϕ bits. Then, real-valued Givens rotations are utilised to successively zero out the second to the KM -th element of the first column of $\mathbf{F}^{[k]}$. For the latter rotations the angles $\psi_{2,1}, \dots, \psi_{KM,1}$ are used. The angles lie between 0 and $\pi/2$ and are quantised uniformly with b_ψ bits. This procedure is repeated in a similar fashion for the remaining columns of $\mathbf{F}^{[k]}$. More details are presented in [31] and [32] as well as in the Matlab/Octave functions available at <http://people.kth.se/~perz/packV/>.

Since we use OFDM there is one $\mathbf{H}^{[k]}$ matrix for each user and sub-carrier. In the IEEE 802.11ac standard, the parameter N_g is defined. This parameter determines the frequency domain granularity of the feedback. If $N_g = 1$, the feedback of $\mathbf{F}^{[k]}$ is done on every sub-carrier. If $N_g = 2$, the feedback is only done on every other sub-carrier. In the standard, the values 1, 2 and 4 have been defined for N_g . In our measurements the values 8, 16 and 38 have also been considered, since this would significantly reduce the number of feedback bits. The angle resolution parameters b_ϕ and b_ψ are defined in the IEEE 802.11ac standard as either $b_\phi = 5$ and $b_\psi = 7$ or $b_\phi = 7$ and $b_\psi = 9$. In the presented results only the latter value pair is used. The total number of bits required to feed back the $\mathbf{F}^{[k]}$ matrix is given by

$$n_b = ((2KM - 1)M - M^2)(b_\phi + b_\psi)/2 \quad (28)$$

The number of bits can be reduced by a further $(K - 1)b_\phi$ bits. We can see this by dividing the $\mathbf{F}^{[k]}$ into sub-matrices of size $M \times M$ as

$$(\mathbf{F}^{[k]})^* = [(\mathbf{F}_1^{[k]})^*, \dots, (\mathbf{F}_K^{[k]})^*]. \quad (29)$$

Since the signals from source, l , only propagates through sub-matrix $\mathbf{F}^{[k]}_l$, we may freely multiply sub-matrices $1, \dots, K - 1$ by one phasor each. By doing so, we may set $\phi_{1,1}, \dots, \phi_{1+(K-2)M,1}$ to zero, and thus we do not need to transmit them over the feedback channels. The last sub-matrix can not be rotated since then the last row of $\mathbf{F}^{[k]}$ would no longer be real and positive.

The elements of $\mathbf{\Lambda}^{[k]}$ are divided by the noise standard deviation. The so obtained value can be regarded as the SNR of a corresponding stream. The reporting of these SNRs are done separately per stream, and is done in two steps. In the first step, the average SNR in dB over the whole frequency band, i.e. for all singular values of the narrowband channels for which SNR is reported, is fed back to S_k . This value is uniformly quantised with 8 bits in the range from 10 dB to 53.75 dB. In the second step, the difference in dB between the SNR of the reported sub-carrier and the average SNR is computed and is uniformly quantised with 4 bits in the range from 8 dB to 7 dB. In S_k , the SNRs of all the reported sub-carriers are first reconstructed. Then, linear interpolation (in dB) is deployed to obtain the SNR for all the sub-carriers for which $\mathbf{F}^{[k]}$ is fed back. With these two entities at hand, the channel matrices $\mathbf{H}^{[k]}$ are reconstructed and used to compute the desired pre-coders. For the sub-carriers where there is no feedback available, the pre-coding of the nearest reported sub-carrier is utilized, i.e. no matrix interpolation method is used.

A practical problem which occurred during the early experimentation was that the SNR sometimes exceeded 53.75dB. This happened due to the high transmission power and short range. First this was handled by reporting the maximum value 53.75dB whenever this happened. However, this resulted in making the reconstructed channel at the transmitter high-rank although the estimated channel at the receiver were in fact low-rank - which was very detrimental to the performance. To circumvent this problem, an offset is subtracted from SNR values when this condition happens.

B. Results

In addition to interference alignment ², we also run the reference scheme single-user MIMO. In this scheme two spatial streams are transmitted from each source using its two transmitter antennas. Two versions of the single-user MIMO is used. In one version one source is active at a time. This version is naturally called TDMA. In another version of single-user MIMO all links are active at the same time. This scheme will work well if the inter-link interference is weak. We call this approach *full-reuse MIMO*. Finally, we also include a scheme called *full-reuse SIMO*. In this approach all sources transmit at the same time but using only a single-antenna at the sources. The difference between this scheme and interference alignment is the beamforming at the sources and the channel state feedback. All other aspects of the signal processing are identical. The performance of the system were investigated in 43 different locations for each of the three destination terminals. Half of the locations were in the corridor and half in the adjacent rooms, see Figure 5. In each location the performance was investigated with the frequency domain granularity parameter, N_g set sequentially to the values 1, 2, 4, 8, 15, 38. No person or object was moving in the environment and all schemes were run in rapid sequence thus making it possible to reliably compare the results. The results are shown in Figure 8. The dashed lines are the results obtained without the feedback compression while the solid lines are with compression (although the frequency domain granularity is still applied). The

²By interference alignment we are here referring to the modified form of interference alignment known as Max-SINR, see Section III-C. However, measurements we have performed has shown that the performance difference between the original interference alignment and Max-SINR is negligible in our scenario.

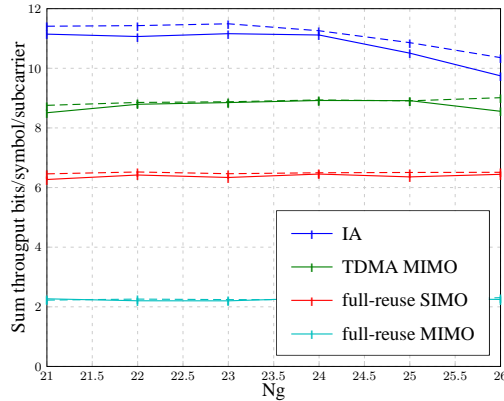


Fig. 8: Measured sum throughput. The dotted line are the results without compression

results show negligible performance loss from the quantization. However, using a too high frequency domain granularity, $N_g > 8$ or 2.5MHz, do incur some loss. Note that the result for full-reuse MIMO is very poor showing that the interference is strong. The gain of interference alignment over the best reference scheme (TDMA MIMO) is 27%. We may also note that interference alignment provides a gain over full-reuse SIMO which proves that the transmitter beamforming is making a difference.

When the channel is changing the performance of interference alignment will inevitably be degraded due the channel mismatch between the channel at the feedback time and the channel at the actual transmission. The amount of degradation depends on the time delay and the level of movement in the environment. In [26] using measurements we showed that the throughput of interference alignment dropped 6.4% when two passers-by were walking in the measurement environment and the feedback delay interval was 23 ms. With this delay interval the overhead of performing the feedback scheme above with $N_g = 8$ is 2.5%, assuming that the feedback scheme of IEEE802.11ac is used.

The channel may also change due to the existence of the users at the destinations. This effect was studied by measuring the performance with and without a user located close to the destination nodes. The results were obtained using eight destination positions. The performance of interference alignment dropped 4.9% while the performance of single-user MIMO was unaffected.

These results show that interference alignment can still deliver a net performance gain of sum throughput some 15% over single-user MIMO in a WiFi scenario with three access points and three users, even when feedback overheads and mobility is taken into account.

VIII. CONCLUSION

We have reviewed the concept of interference alignment, with theoretical results regarding power and time allocation between training and payload data transmission, and previous works within experimentation on interference alignment. We further present implementation efforts addressing the combination of iterative interference alignment and power control and using compressed channel state feedback based on a modified form of the MU-MIMO feedback scheme of IEEE802.11ac. Our experimental results show that the iterative interference alignment and power control scheme is able to provide better FER/BER performance (16QAM code rate 0.5), than an implementation without power control. The results using the modified IEEE802.11ac feedback scheme, show that interference alignment can bring an improvement in throughput when considering the loss of bandwidth needed for feedback of the channel state information even for channels with realistic indoor mobility.

IX. ACKNOWLEDGMENTS

The research leading to these results has received funding from Swedish Foundation for Strategic Research (SSF) under RAMCOORAN project and ACCESS Linnaeus Center under graduate course wireless experimentations. The measurements were performed within the framework of the HIATUS project. The project HIATUS acknowledges the financial support of the Future and Emerging Technologies (FET) programme within the Seventh Framework Programme for Research of the European Commission under FET-Open grant number: 265578.

REFERENCES

- [1] A. Osseiran, V. Braun, T. Hidekazu, P. Marsch, H. Schotten, H. Tullberg, M. A. Uusitalo, and M. Schellman, "The foundation of the mobile and wireless communications system for 2020 and beyond challenges, enablers and technology solutions," in *IEEE Vehicular Technology Conference (VTC'13)*, 2013.
- [2] V. Tarokh, N. Seshadri, and A. R. Calderbank, "Space-time codes for high data rate wireless communication: performance criterion and code construction," *IEEE Transactions on Information Theory*, vol. 44, pp. 744–765, Mar. 1998.
- [3] M. A. Maddah-Ali, A. S. Motahari, and A. K. Khandani, "Communication over MIMO X channels: Interference alignment, decomposition, and performance analysis," *IEEE Transactions on Information Theory*, vol. 54, pp. 3457–3470, Aug. 2008.
- [4] V. R. Cadambe and S. A. Jafar, "Interference alignment and degrees of freedom of the K -user interference channel," *IEEE Transactions on Information Theory*, vol. 54, pp. 3425–3441, Aug. 2008.
- [5] O. E. Ayach, S. W. Peters, and R. J. Heath, "The practical challenges of interference alignment," *IEEE Transactions on Wireless Communications*, vol. 20, no. 1, pp. 35–42, 2013.
- [6] H. Maleki, S. A. Jafar, and S. Shamai, "Retrospective interference alignment over interference networks," *IEEE Journal of Selected Topics in Signal Processing*, vol. 6, pp. 228–240, June 2012.
- [7] M. A. Maddah-Ali and D. Tse, "Completely stale transmitter channel state information is still very useful," in *48th Annual Allerton Conference on Communication, Control, and Computing (Allerton'10)*, Sept. 2010.
- [8] B. Nazer, S. Jafar, M. Gaspar, and S. Vishwanath, "Ergodic interference alignment," in *IEEE International Symposium on Information Theory (ISIT'09)*, (Seoul, Korea), June 2009.
- [9] R. Brandt, H. Asplund, and M. Bengtsson, "Interference alignment in frequency - a measurement based performance analysis," in *Systems, Signals and Image Processing (IWSSIP), 2012 19th International Conference on*, pp. 227–230, 2012.
- [10] A. S. Motahari, S. O. Gharan, M. A. Maddah-Ali, and A. K. Khandani, "Real interference alignment: Exploiting the potential of single antenna systems," Nov. 2009.
- [11] R. Brandt, P. Zetterberg, and M. Bengtsson, "Interference alignment over a combination of space and frequency," in *Communications Workshops (ICC), 2013 IEEE International Conference on*, pp. 149–153, June 2013.
- [12] H. Farhadi, M. N. Khormuji, and M. Skoglund, "Pilot-assisted ergodic interference alignment for wireless networks," in *IEEE International Conference on Acoustics, Speech and Signal Processing (ICASSP'14)*, (Florence, Italy), May 2014.
- [13] H. Farhadi, M. N. Khormuji, C. Wang, and M. Skoglund, "Ergodic interference alignment with noisy channel state information," in *IEEE International Symposium on Information Theory Proceedings (ISIT'13)*, (Istanbul, Turkey), Jul. 2013.
- [14] H. Bolcskei and I. J. Thukral, "Interference alignment with limited feedback," in *IEEE International Symposium on Information Theory (ISIT'09)*, (Seoul, Korea), June 2009.
- [15] R. T. Krishnamachari and M. K. Varanasi, "Interference alignment under limited feedback for MIMO interference channels," in *IEEE International Symposium on Information Theory (ISIT'10)*, (Austin, Texas, U.S.A), June 2010.
- [16] J. S. Kim, S. H. Moon, S. R. Lee, and I. Lee, "A new channel quantization strategy for MIMO interference alignment with limited feedback," *IEEE Transactions on Wireless Communications*, vol. 11, pp. 358–366, Jan. 2012.
- [17] K. Gomadam, V. R. Cadambe, and S. A. Jafar, "A distributed numerical approach to interference alignment and applications to wireless interference networks," *IEEE Transactions on Information Theory*, vol. 57, pp. 3309 – 3322, June 2011.
- [18] S. Gollakota, S. D. Perli, and D. Katabi, "Interference alignment and cancellation," in *In Proceedings of ACM SIGCOMM*, 2009.
- [19] O. El Ayach, S. Peters, and R. Heath, "The feasibility of interference alignment over measured MIMO-OFDM channels," *Vehicular Technology, IEEE Transactions on*, vol. 59, pp. 4309–4321, Nov 2010.
- [20] P. Zetterberg and N. Moghadam, "An experimental investigation of SIMO, MIMO, interference-alignment (IA) and coordinated multi-point (CoMP)," in *Systems, Signals and Image Processing (IWSSIP), 2012 19th International Conference on*, pp. 211–216, April 2012.

- [21] O. Gonzalez, D. Ramirez, I. Santamaria, J. Garcia-Naya, and L. Castedo, "Experimental validation of interference alignment techniques using a multiuser MIMO testbed," in *Smart Antennas (WSA), 2011 International ITG Workshop on*, pp. 1–8, Feb 2011.
- [22] J. Massey, J. Starr, S. Lee, D. Lee, A. Gerstlauer, and R. Heath, "Implementation of a real-time wireless interference alignment network," in *Signals, Systems and Computers (ASILOMAR), 2012 Conference Record of the Forty Sixth Asilomar Conference on*, pp. 104–108, Nov 2012.
- [23] M. Mayer, G. Artner, G. Hannak, M. Lerch, and M. Guillaud, "Measurement based evaluation of interference alignment on the vienna MIMO testbed," in *Wireless Communication Systems (ISWCS 2013), Proceedings of the Tenth International Symposium on*, pp. 1–5, Aug 2013.
- [24] N. N. Moghadam, H. Farhadi, P. Zetterberg, and M. Skoglund, "Test-bed implementation of iterative interference alignment and power control for wireless MIMO interference networks," in *IEEE International Workshop on Signal Processing Advances in Wireless Communications (SPAWC'14)*, (Toronto, Canada), Jun 2014.
- [25] P. Zetterberg, "Interference alignment (IA) and coordinated multi-point (CoMP) with IEEE802.11ac feedback compression: testbed results," 2014.
- [26] P. Zetterberg, "Interference alignment (IA) and coordinated multi-point (CoMP) with IEEE802.11ac feedback compression: testbed results," in *IEEE Vehicular Technology Conference*, 2014.
- [27] H. Farhadi, C. Wang, and M. Skoglund, "Distributed interference alignment and power control for wireless MIMO interference networks," in *IEEE Wireless Communications and Networking Conference (WCNC13)*, (Shanghai, China), Apr. 2013.
- [28] R. Yates, "A framework for uplink power control in cellular radio systems," *Selected Areas in Communications, IEEE Journal on*, vol. 13, pp. 1341–1347, Sep 1995.
- [29] H. Farhadi, A. Zaidi, C. Fischione, C. Wang, and M. Skoglund, "Distributed interference alignment and power control for wireless MIMO interference networks with noisy channel state information," in *IEEE International Black Sea Conference on Communications and Networking (BlackSeaCom'13)*, (Batumi, Georgia), 2013.
- [30] T. Schenk, *RF Imperfections in High-rate Wireless Systems*. Springer Netherlands, 2008.
- [31] J. Roh and B. Rao, "Efficient feedback methods for MIMO channels based on parameterization," *IEEE Transactions on Wireless Communications*, vol. 6, no. 1, pp. 282–292, 2007.
- [32] R. Porat, E. Ojard, N. Jindal, M. Fischer, and V. Erceg, "Improved MU-MIMO performance for future 802.11 systems using differential feedback," in *UCSD Information Theory and Applications Workshop*, (Catamaran Resort, San Diego, USA), pp. 1–5, 2013.